HIP-2004-38/TH
SPhT-T04/111
hep-ph/0409058

Quark-antiquark production from classical fields in heavy ion collisions: 1+1 dimensions

F. Gelis[a] [1], K. Kajantie[b] [2], T. Lappi[b,c] [3].

[a] *Service de Physique Theorique, Bât. 774, CEA/DSM/Saclay, 91191 Gif-sur-Yvette, France*
[b] *Department of Physics, P.O.Box 64, FIN-00014 University of Helsinki, Finland*
[c] *Helsinki Institute of Physics, P.O.Box 64, FIN-00014 University of Helsinki, Finland*

Classical color fields produced by the small-x wave functions of colliding ultrarelativistic nuclei have been numerically computed. We set up the framework for computing the production of small-mass quark-antiquark pairs in these color fields by numerically integrating the Dirac equation. This computation is essential for understanding the conversion of the initial gluonic state to chemically equilibrated quark-gluon plasma. To illustrate and overcome technical difficulties associated with the longitudinal dimension, we first consider numerically the case of one time + one longitudinal space dimension.

[1] fgelis@cea.fr
[2] keijo.kajantie@helsinki.fi
[3] tuomas.lappi@helsinki.fi

1 Introduction

The dynamics of an ultrarelativistic heavy ion collisions is usually described in the following terms: two nuclei in their $T = 0$, entropy=0 ground state move along the light cone, collide at $t = 0$ and form a large-entropy extended system with deconfined quark-gluon degrees of freedom. This system expands, passes a QCD phase transition, converts itself to a hadronic phase, which finally decouples and sends hadrons to detectors.

Important partial confirmation for this scenario comes from recent experimental results from the relativistic heavy ion collider RHIC. These suggest that in $\sqrt{s} = 200$ GeV Au+Au collisions a nearly thermalised quark-gluon plasma is formed [1]. One of the main pieces of evidence comes from azimuthal asymmetries in non-central collisions [2, 3, 4]: a hydrodynamic computation [5], with an assumed equation of state and initial conditions fitted to transverse spectra, shows that the initial spatial azimuthal asymmetry is converted to just the correct amount of momentum space azimuthal asymmetry if the equation of state is that of an ideal fluid.

There is one significant deficiency in the theoretical analysis of this scenario: virtually all the models describing the initial state (for examples, see [6, 7, 8, 9, 10]) are based on the almost purely gluonic small-x partonic content of the nuclear wave function, while an ideal quark-gluon plasma would contain gluons and quarks+antiquarks in the ratio $16/(21N_f/2)$ and anyway the final hadronic state contains flavour in a fully thermalised manner [11]. At what stage do the small-mass u,d, and s flavour degrees of freedom appear in the system? Experiments do not yet shed any light on this problem.

Models based on weakly coupled quark-gluon degrees of freedom, like parton cascade models, fail to reproduce both kinetic and chemical equilibration [12]; the coupling is so weak that collision times become too large relative to the lifetime of the system. The purpose of this paper is to start from a strongly coupled and phenomenologically viable model, the classical field computation of gluon production in a collision of two nuclei [7, 13, 14] using the McLerran-Venugopalan model [8] for the distribution of gluons in a single nucleus, later evolved and termed color glass condensate (see [15] and references therein). We then discuss how the amount of small-mass u,d, and s quark-antiquark pairs produced by the colour fields of this model can be computed by numerically integrating the evolution of a negative energy spinor as given by the Dirac equation and projecting on a positive energy spinor[16, 17]. In this paper we give numerical results only for a 1+1 dimensional toy model version of the full computation, to establish the viability of the method.

The following should be emphasised from the outset:

- This is not a computation of pair production from strong colour fields by quantum tunneling via the Schwinger mechanism, which has often been studied [18, 19]. Instead, the pairs are produced via multiple interactions of quasi-real Fourier components of the color fields; in the dilute limit this is just the two gluon fusion mechanism $g^\star+g^\star \rightarrow q+\bar{q}$, which for heavy quarks also is the dominant mechanism [20]. The same produc-

tion mechanism has been studied in [21], where several approximations for the quark retarded propagator in an external field have been investigated.

- Basically, there are two quantities we would like to know: how fast does the $\mathrm{q\bar{q}}$ density grow in comparison with the gluon density (what are the typical production times in units of $1/Q_s$, Q_s = saturation scale, see below) and how high is the $\mathrm{q\bar{q}}$ density in comparison with the gluon density (what are the total energies per unit rapidity in units of $R_A^2 Q_s^3$). Parametrically, quark pair production is suppressed by a factor α_s, but we are not in the weak coupling limit. In the strong coupling regime, a large $\mathrm{q\bar{q}}$ component could be created, as required for chemical equilibration. Kinetic equilibration of the longitudinal degree of freedom is still an open issue.

- The pair production being computed in a given colour field, the feedback is not taken into account. The results will thus be quantitatively reliable only as long as the energy in $\mathrm{q\bar{q}}$ pairs remains less than that in gluons. For the Abelian Higgs model in 1+1 dimensions and with different initial conditions a numerical scheme for including both bosonic and fermionic dynamical degrees of freedom has been developed in [22].

- The computation of the $\mathrm{q\bar{q}}$ production is technically much more complicated than that of gluons. The colour fields giving rise to gluons are assumed to be independent of the space-time rapidity $\eta = \frac{1}{2}\log(x^+/x^-)$, they only depend on $\tau, \mathbf{x}_T$. Thus strict boost invariance for gluons is obtained (unless rapidity dependence is introduced via that of the saturation scales) and the single rapidity of the problem, that of the gluon, can be completely removed from the equations. For quark pair production, two rapidities enter and a non-trivial dependence in $\Delta y = y_\mathrm{q} - y_\mathrm{\bar{q}}$ appears. This also implies that the quark wave function $\psi(\tau, \eta, \mathbf{x}_T)$ will depend on all the 3+1 variables. However, formulating the initial condition on the light cones (say, $x^- = 0, x^+ > 0$) is impossible using the natural variables τ, η since fixed $x^+ = \tau\exp(\eta)/\sqrt{2} > 0$ cannot be reached for $\tau \to 0$ unless also $\eta \to \infty$. We thus have to use as variables $\tau, x^\pm$ or, more symmetrically, τ, z.

- For an approach to quark pair production via special nonperturbative instanton configurations, see [23].

The structure of this paper is as follows. In section 2 the problem is formulated in full generality in 3+1 dimensions. Particular attention is given to the initial condition and the difficulties associated with the longitudinal dimension are pointed out. This leads us to truncate the full theory by neglecting all the transverse integrations to a 1+1 dimensional toy model, with which we can test the numerical solution of the time+longitudinal dependence. The free Dirac equation in 1+1 dimensions using (τ, η), $(\tau, x^\pm)$ or (τ, z) as variables (we do not go all the way to (t, z)!) is studied and solved analytically in section 3. Its numerical solution is carried out in section 4 and shown to agree with the analytic one. Finally, in

section 5 the 1+1 dimensional Dirac equation is solved with various forms of the external gluonic field.

In the time-longitudinal space we shall use three sets of variables: t, z, $\mathrm{d}s^2 = \mathrm{d}t^2 - \mathrm{d}z^2$, the light cone coordinates $x^\pm = (t \pm z)/\sqrt{2} = \tau e^{\pm\eta}/\sqrt{2}$, $\mathrm{d}s^2 = 2\mathrm{d}x^+\mathrm{d}x^-$ and proper time and spacetime rapidity $\tau = \sqrt{t^2 - z^2} = \sqrt{2x^+x^-}$, $\eta = \frac{1}{2}\ln(x^+/x^-)$, $\mathrm{d}s^2 = \mathrm{d}\tau^2 - \tau^2\mathrm{d}\eta^2$. For any four-vector A_μ we have as $A_\tau = A^\tau = (tA^0 - zA^3)/\tau = (x^+A^- + x^-A^+)/\tau$ and $A_\eta = -\tau^2 A^\eta = zA^0 - tA^3 = x^+A^- - x^-A^+$. This also applies to Dirac gamma matrices, giving $\gamma^\tau = \gamma^0 e^{-\eta\gamma^0\gamma^3}$. We shall frequently separate Dirac spinors into eigenvectors of $\gamma^0\gamma^3$, using the projection operators

$$P^\pm = \frac{1}{2}(1 \pm \gamma^0\gamma^3) = \frac{1}{\sqrt{2}}\gamma^0\gamma^\pm = \frac{1}{\sqrt{2}}\gamma^\mp\gamma^0 = \frac{1}{2}\,\gamma^\mp\gamma^\pm, \tag{1}$$

satisfying $P^\pm P^\pm = P^\pm$, $P^\pm P^\mp = 0$, $P^+ + P^- = 1$. For momenta we use the transverse mass $\omega_p \equiv \mathbf{p}_T{}^2 + m^2$ and rapidity $y = \frac{1}{2}\ln(p^+/p^-)$, giving the energy $E_p = \omega_p \cosh y$ and the longitudinal momentum $p^z = \omega_p \sinh y$.

2 General formulation of the problem in 3+1 dimensions; initial conditions on the light cone

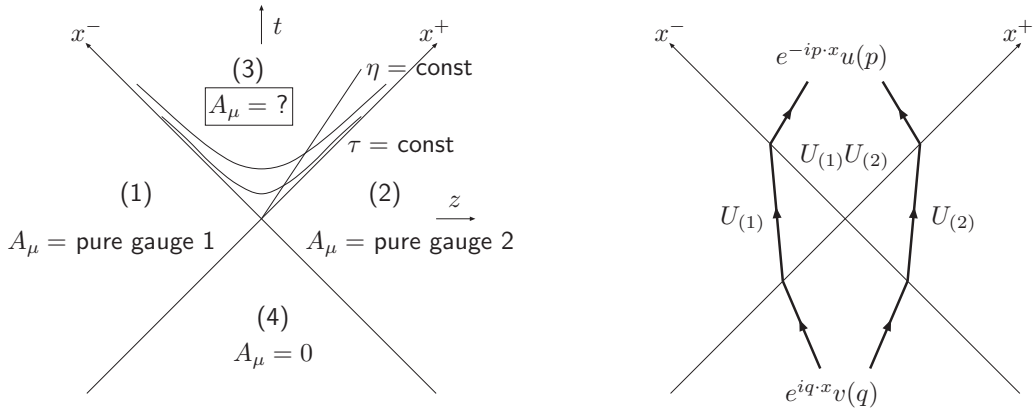

Figure 1: Left: The background gauge field from the classical field model. In the Abelian case the field is a pure gauge also in region (3). Right: The two possible trajectories of (retarded) propagation of the fermion. The spinor starts from a negative energy state $e^{iq\cdot x}v(q)$ and gets a k^+-kick from the gluon field (1) on the x^+-axis and then a k^--kick from the gluon field (2) on the x^--axis; or in the other order. Finally the spinor is projected onto positive energy states $e^{-ip\cdot x}u(p)$ inside the future light cone. The label $U_{(1)}U_{(2)}$ refers only to the Abelian case, when the pure gauge field inside the future light cone is given by $U_{(1)}U_{(2)} = U_{(2)}U_{(1)}$.

We want to calculate the number of quark-antiquark pairs produced by the classical color fields in the model developed in Refs. [7, 8] and solved numerically in Refs. [13, 14]. In [17], it was shown that the average number of produced pairs can be expressed as follows:

$$\begin{aligned}\langle n_{q\bar{q}}\rangle &= \int \frac{d^3\mathbf{p}}{(2\pi)^3 2E_p}\Big\langle 0_{\rm in}\Big|b^\dagger_{\rm out}(\mathbf{p})b_{\rm out}(\mathbf{p})\Big|0_{\rm in}\Big\rangle \\ &= \int \frac{d^3\mathbf{p}}{(2\pi)^3 2E_p}\int \frac{d^3\mathbf{q}}{(2\pi)^3 2E_q}\Big|\overline{u}(p)\mathcal{T}_{_R}(p,-q)v(q)\Big|^2, \end{aligned} \tag{2}$$

where $\mathcal{T}_{_R}(p,-q)$ is the amputated retarded propagator of the quark in the external field, $-q$ and p being respectively the incoming and outgoing momenta. Note that this quantity is distinct from the cross-section to produce one pair, which would require the time-ordered propagator of the quark. The difference between the two cases is explained in more detail in [17]. For computational purposes, it is in fact more convenient to write the previous formula in coordinate space. This can be achieved by using the standard machinery of reduction formulas, and one obtains:

$$\overline{u}(p)\mathcal{T}_{_R}(p,-q)v(q) = \lim_{x_0\to+\infty}\int d^3\mathbf{x}e^{i(E_p x^0-\mathbf{p}\cdot\mathbf{x})}u^\dagger(p)\psi_{\mathbf{q}}(x^0,\mathbf{x}), \tag{3}$$

where $\psi_{\mathbf{q}}(x^0,\mathbf{x})$ is the solution of the Dirac equation in the presence of the external field, with a negative energy free spinor as its initial boundary value:

$$\psi_{\mathbf{q}}(x^0\to-\infty,\mathbf{x}) = e^{i(E_q x^0-\mathbf{q}\cdot\mathbf{x})}v(q). \tag{4}$$

This formula can be trivially modified in order to use the proper time τ instead of x^0. Moreover, although it tells us that the on-shell pair production amplitude is obtained only in the limit of infinite time, one can also consider an extension of this formula where the limit is not taken, thereby defining a "time dependent pair-production amplitude" which could be used in order to probe the typical time-scale necessary to produce the fermions. We shall give several examples of this below (see Fig. 6 and Fig. 7).

Note that in this formalism, one neglects the backreaction of the produced fermions on the color field. It is therefore a good approximation only if the fermions do not outnumber the gluons. In an Abelian theory the calculation only involves pure gauge fields and the pair production amplitude (see Eq. (15) below) can be calculated analytically[4], as shown in [16]. Furthermore, in an Abelian theory, the square of this generalized amplitude is, in fact, time-independent, suggesting that all the pairs are produced instantaneously at the collision time (for a collision at infinite energy).

In the non-Abelian case the gauge fields are known analytically up to the future light cone ($\tau = 0$) and numerically for $\tau \geq 0$. Thus we will have to solve the Dirac equation numerically

[4]However, the evaluation of this amplitude is complicated by some infrared singularities that need to be properly regularized [24].

for that region, with the initial condition at $\tau = 0$ given by essentially the same calculation as in the Abelian case.

Let us first review the classical field model of [7, 8]. Then we shall repeat the calculation of fermion-antifermion production from Abelian Weizsäcker-Williams fields from Ref. [16] and use it to find the initial conditions at $\tau = 0$ for our numerical calculation in the non-Abelian case.

Let us assume we have two nuclei moving along the light cone, corresponding to a current

$$J^\mu = \delta^{\mu+}\delta(x^-)\rho_{(1)}(\mathbf{x}_T) + \delta^{\mu-}\delta(x^+)\rho_{(2)}(\mathbf{x}_T). \tag{5}$$

The two colour charge densities $\rho_{(m)}(\mathbf{x}_T)$ are, independently for the two nuclei, drawn from a random ensemble, which in the original McLerran-Venugopalan model is taken to be Gaussian:

$$\langle \rho^a_{(m)}(\mathbf{x}_T)\rho^b_{(m)}(\mathbf{y}_T)\rangle = g^2\mu^2_{(m)}\delta^{ab}\delta^2(\mathbf{x}_T - \mathbf{y}_T), \quad m = 1, 2, \tag{6}$$

where μ is a parameter describing the transverse density of color charges and can be related, up to a logarithmic uncertainty, to the saturation scale Q_s [25]. More generally the charge distribution in Eq. (6) is not known, but its evolution when probing smaller Feynman x values in the nuclei can be calculated from the JIMWLK equation, see e.g. [26].

One first calculates in the light cone gauge ($A^+ = 0$ for the nucleus moving in the $+z$ direction, and $A^- = 0$ for the nucleus moving in the $-z$ direction) the pure gauge fields corresponding two the two nuclei:

$$A^i_{(m)}(\mathbf{x}_T) = \frac{i}{g}U_{(m)}(\mathbf{x}_T)\partial_i U^\dagger_{(m)}(\mathbf{x}_T), \quad m = 1, 2. \tag{7}$$

These depend on the Wilson lines $U_{(m)}(\mathbf{x}_T)$ given by

$$U_{(m)}(\mathbf{x}_T) = \exp\left(-ig\frac{\rho_{(m)}}{{\boldsymbol{\nabla}_T}^2}(\mathbf{x}_T)\right). \tag{8}$$

In a temporal gauge[5] $A_\tau = 0$ the initial condition at $\tau = 0$ for the color fields $\mathbf{A}_T(\tau, \mathbf{x}_T)$ and $A_\eta(\tau, \mathbf{x}_T)$ is given by these pure gauge fields corresponding to the two nuclei:

$$\begin{aligned} A^i(0, \mathbf{x}_T) &= A^i_{(1)}(\mathbf{x}_T) + A^i_{(2)}(\mathbf{x}_T), \\ A^\eta(0, \mathbf{x}_T) &= \frac{ig}{2}[A^i_{(1)}(\mathbf{x}_T), A^i_{(2)}(\mathbf{x}_T)]. \end{aligned} \tag{9}$$

One then solves the equations of motion

$$[D_\mu, F^{\mu\nu}] = 0 \tag{10}$$

[5]The $A_\tau = 0$ gauge coincides with the light-cone gauge $A^+ = 0$ (resp. $A^- = 0$) if $x^+ = 0$ (resp. $x^- = 0$). This is why we can use the gauge field of the nuclei before the collision, in two different light-cone gauges, as an initial condition at $\tau = 0$ for the gauge field in the $A_\tau = 0$ gauge.

using these initial conditions to find the fields at later times $\tau > 0$. In this gauge it is easy to find the Hamiltonian and thus the energy of a given field configuration. Additionally, fixing the Coulomb gauge in the transverse plane, $\boldsymbol{\nabla}_T \cdot \mathbf{A}_T = 0$, one can also define a multiplicity corresponding to the classical fields.

Let us then turn to solving the Dirac equation in the Abelian case, following [16]. In [16] it is solved separately in different gauges, covariant gauge (called singular gauge in [16]) and light-cone gauge. In [20] the covariant gauge is used. Here we use the light-cone gauge, because it is the same gauge that was used in solving the Yang-Mills equations up to the $\tau = 0$ light cone.

Following Eqs. (3) and (4) we start with a negative energy plane wave for $x^{\pm} < 0$:

$$\psi_{(4)}(x) = e^{iq\cdot x} v(q). \tag{11}$$

The boundary conditions when crossing the light cones can be derived from the following argument. Since $\gamma^+ P^- = \gamma^- P^+ = 0$, the Dirac equation only involves terms like $\partial_- P^- \psi$ and $\partial_+ P^+ \psi$, but not $\partial_- P^+ \psi$ and $\partial_+ P^- \psi$. If there were a discontinuity in $P^- \psi$ on the $x^- = 0$ light cone, the derivative term would give a delta function, with no other term to compensate it, which is not possible. A discontinuity in $P^+ \psi$, on the other hand, is possible because it can be compensated by the $\theta(x^-)$-discontinuity in the gauge field. Thus the boundary condition is that on the $x^{\pm} = 0$ light cone $\psi^{\pm}$ is continuous. Using this boundary condition one can find the solutions in the regions (1) ($x^- > 0 > x^+$) and (2) ($x^+ > 0 > x^-$):

$$\begin{aligned}
\psi_{(1)}(x) &= U_{(1)}(\mathbf{x}_T) \int \frac{\mathrm{d}^2\mathbf{k}_T}{(2\pi)^2} U^\dagger_{(1)}(\mathbf{k}_T - \mathbf{q}_T) e^{-i\mathbf{k}_T\cdot\mathbf{x}_T} \\
&\quad \times \exp\left(iq^- x^+ + i\frac{\omega_k^2}{2q^-} x^- \right) \left[P^- + P^+ \gamma^0 \frac{\boldsymbol{\gamma}_T \cdot \mathbf{k}_T - m}{\sqrt{2} q^-} \right] v(q) \,, \\
\psi_{(2)}(x) &= U_{(2)}(\mathbf{x}_T) \int \frac{\mathrm{d}^2\mathbf{k}_T}{(2\pi)^2} U^\dagger_{(2)}(\mathbf{k}_T - \mathbf{q}_T) e^{-i\mathbf{k}_T\cdot\mathbf{x}_T} \\
&\quad \times \exp\left(i\frac{\omega_k^2}{2q^+} x^+ + iq^+ x^- \right) \left[P^+ + P^- \gamma^0 \frac{\boldsymbol{\gamma}_T \cdot \mathbf{k}_T - m}{\sqrt{2} q^+} \right] v(q) \,,
\end{aligned} \tag{12}$$

where $\omega_k^2 \equiv {\mathbf{k}_T}^2 + m^2$ and we have defined the Fourier transforms as:

$$U^\dagger_{(m)}(\mathbf{k}_T) \equiv \int \mathrm{d}^2\mathbf{y}_T e^{i\mathbf{y}_T\cdot\mathbf{k}_T} U^\dagger_{(m)}(\mathbf{y}_T). \tag{13}$$

Next we must continue to the forward light cone. The solution that matches to Eq. (12)

on the light cone is

$$\begin{aligned}
\psi_{(3)}(x) &= U_{(1)}(\mathbf{x}_T)U_{(2)}(\mathbf{x}_T)\int\frac{\mathrm{d}^2\mathbf{p}_T}{(2\pi)^2}\frac{\mathrm{d}^2\mathbf{k}_T}{(2\pi)^2}\left[\frac{\mathrm{d}p^+}{2\pi i}\frac{1}{p^+-\frac{\omega_k^2}{2q^-}-i\epsilon}\right]e^{-i\mathbf{p}_T\cdot\mathbf{x}_T}\\
&\quad\times\exp\left(i\frac{\omega_p^2}{2p^+-i\epsilon}x^+ + ip^+x^-\right)U^\dagger_{(2)}(\mathbf{p}_T-\mathbf{k}_T)U^\dagger_{(1)}(\mathbf{k}_T-\mathbf{q}_T)\\
&\quad\times\left[P^+ + P^-\gamma^0\frac{\boldsymbol{\gamma}_T\cdot\mathbf{p}_T-m}{\sqrt{2}p^+-i\epsilon}\right]\gamma^0\frac{\boldsymbol{\gamma}_T\cdot\mathbf{k}_T-m}{\sqrt{2}q^-}v(q)\\
&\quad+U_{(1)}(\mathbf{x}_T)U_{(2)}(\mathbf{x}_T)\int\frac{\mathrm{d}^2\mathbf{p}_T}{(2\pi)^2}\frac{\mathrm{d}^2\mathbf{k}_T}{(2\pi)^2}\left[\frac{\mathrm{d}p^-}{2\pi i}\frac{1}{p^--\frac{\omega_k^2}{2q^+}-i\epsilon}\right]e^{-i\mathbf{p}_T\cdot\mathbf{x}_T}\\
&\quad\times\exp\left(i\frac{\omega_p^2}{2p^--i\epsilon}x^- + ip^-x^+\right)U^\dagger_{(1)}(\mathbf{p}_T-\mathbf{k}_T)U^\dagger_{(2)}(\mathbf{k}_T-\mathbf{q}_T)\\
&\quad\times\left[P^- + P^+\gamma^0\frac{\boldsymbol{\gamma}_T\cdot\mathbf{p}_T-m}{\sqrt{2}p^--i\epsilon}\right]\gamma^0\frac{\boldsymbol{\gamma}_T\cdot\mathbf{k}_T-m}{\sqrt{2}q^+}v(q)\,. \qquad (14)
\end{aligned}$$

Here the first term corresponds to a situation in which the positron state q first hits the nucleus 1 moving in the x^+ direction, propagates over region 1, meets the nucleus 2 and propagates into region 3 (the branch on the left in Fig. 1). For QED the order of the $U_{(m)}$ matrices is irrelevant, not so for QCD. The $p^\pm$-integrals in Eq. (14) can be performed to turn the expression into a sum of Bessel functions of the kind we shall encounter in Sec. 3, but we will not write down this complicated expression here.

To find the matrix element for pair production, one has to project the spinor (14) to a positive energy state $e^{-ip\cdot x}u(p)$. Removing the product $U_{(2)}U_{(1)}$, which is a gauge transformation to Coulomb gauge, one gets the Abelian theory result of [16]:

$$\begin{aligned}
M(p,q) = i\sqrt{2}\int\frac{\mathrm{d}^2\mathbf{k}_T}{(2\pi)^2}\Bigg\{&\frac{U^\dagger_{(2)}(-\mathbf{p}_T-\mathbf{k}_T)U^\dagger_{(1)}(\mathbf{k}_T-\mathbf{q}_T)}{\omega_q\omega_p e^{y_p-y_q}+\omega_k^2}u^\dagger(p)\gamma^-\left(\boldsymbol{\gamma}_T\cdot\mathbf{k}_T-m\right)v(q)\\
&+\frac{U^\dagger_{(1)}(-\mathbf{p}_T-\mathbf{k}_T)U^\dagger_{(2)}(\mathbf{k}_T-\mathbf{q}_T)}{\omega_q\omega_p e^{y_q-y_p}+\omega_k^2}u^\dagger(p)\gamma^+\left(\boldsymbol{\gamma}_T\cdot\mathbf{k}_T-m\right)v(q)\Bigg\}. \qquad (15)
\end{aligned}$$

Kinematically, the terms in (15) correspond to the process $k_1+k_2\to p+q$ with $k_1=(p^++q^+,0,\mathbf{k}_T+\mathbf{p}_T)$, $k_2=(0,p^-+q^-,\mathbf{q}_T-\mathbf{k}_T)$ (see Fig. 2). The two terms are the t- and u-channel propagator pole terms in the Feynman diagram corresponding to Fig. 2, with $m^2-t=m^2-(k_1-p)^2=\omega_q\omega_p e^{y_q-y_p}+\omega_k^2$ and $m^2-u=m^2-(k_1-q)^2=\omega_q\omega_p e^{y_p-y_q}+\omega_k^2$.

We now wish to take the Abelian solution for $\tau>0$, Eq. (14), and write it in a form suitable for determining the initial condition as $\tau\to 0$. What is crucial here is the choice of the other variable, kept fixed when taking this limit. The choices are $\eta, z, x^\pm$. To obtain the correct result we must have a dimensionful longitudinal variable, such as z or $x^\pm$ to parametrise

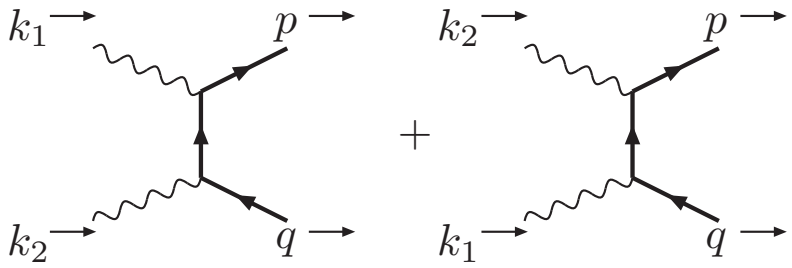

Figure 2: Diagrams contributing to the lowest order pair production amplitude in QED. The incoming photons are quasi-real, with $k_1 = (p^+ + q^+, 0, \mathbf{k}_T + \mathbf{p}_T)$ and $k_2 = (0, p^- + q^-, \mathbf{q}_T - \mathbf{k}_T)$.

the $\tau = 0$ surface. This is because one must be able to represent longitudinal momentum scales, for example $\omega_k^2 e^{y_q}/\omega_q$, in coordinate space. For $\tau > 0$ the corresponding longitudinal coordinate could be constructed as $\tau e^{-\eta}$, but for $\tau = 0$ this is not possible. To enable a symmetric treatment of both branches in Fig. 1, we choose z as the longitudinal variable, with $x^\pm = (\sqrt{\tau^2 + z^2} \pm z)/\sqrt{2} = (|z| \pm z)/\sqrt{2}$ at $\tau = 0$. After a rather lengthy computation, the $\tau \to 0$ limit of the wave function Eq. (14) can be written as

$$
\begin{aligned}
\psi_{(3)}(\tau = 0, z, \mathbf{x}_T) = e^{-i\mathbf{q}_T\cdot\mathbf{x}_T} \int \frac{\mathrm{d}^2\mathbf{k}_T}{(2\pi)^2}\ e^{-i\mathbf{k}_T\cdot\mathbf{x}_T} \\
\times\Bigg\{ P^+ \frac{e^{y_q}}{\omega_q} U_{(1)}(\mathbf{x}_T) U^\dagger_{(1)}(\mathbf{k}_T) \exp\left(i\frac{\omega^2_{k+q} e^{y_q}(|z| - z)}{2\omega_q} \right) \\
+P^- \gamma^0 \left[i\boldsymbol{\gamma}_T\cdot\mathbf{D}_T - m \right] U_{(1)}(\mathbf{x}_T) U^\dagger_{(1)}(\mathbf{k}_T) \frac{1}{\omega^2_{k+q}} \left[\exp\left(i\frac{\omega^2_{k+q} e^{y_q}(|z| - z)}{2\omega_q} \right) - 1 \right] \\
+P^- \frac{e^{-y_q}}{\omega_q} U_{(2)}(\mathbf{x}_T) U^\dagger_{(2)}(\mathbf{k}_T) \exp\left(i\frac{\omega^2_{k+q} e^{-y_q}(|z| + z)}{2\omega_q} \right) \\
+P^+ \gamma^0 \left[i\boldsymbol{\gamma}_T\cdot\mathbf{D}_T - m \right] U_{(2)}(\mathbf{x}_T) U^\dagger_{(2)}(\mathbf{k}_T) \frac{1}{\omega^2_{k+q}} \left[\exp\left(i\frac{\omega^2_{k+q} e^{-y_q}(|z| + z)}{2\omega_q} \right) - 1 \right] \Bigg\} \\
\times\gamma^0 \left(\boldsymbol{\gamma}_T\cdot(\mathbf{k}_T + \mathbf{q}_T) - m \right) v(q),
\end{aligned}
\tag{16}
$$

where $\mathbf{D}_T = \boldsymbol{\nabla}_T + ig\mathbf{A}_T(0, \mathbf{x}_T)$ and $\omega^2_{k+q} = (\mathbf{k}_T + \mathbf{q}_T)^2 + m^2$. Note that whereas Eq. (14) involved products of $U_{(1)}$ and $U_{(2)}$, implicitly assuming that they commute, the terms in Eq. (16) only contain either $U_{(1)}$ or $U_{(2)}$ and thus Eq. (16) can be directly generalised to the non-Abelian theory. The products of $U_{(1)}$ and $U_{(2)}$ show up in the gauge field in the covariant derivative $\mathbf{D}_T$, which depends on both $U_{(1)}$ and $U_{(2)}$ by Eqs. (7),(9).

Now we have the initial conditions for a numerical solution of the Dirac equation in 3+1 dimensions. To proceed further, one will have to generate the random SU(3) matrices $U_{(m)}(\mathbf{x}_T)$, compute the color fields $A_\eta(\tau, \mathbf{x}_T)$, $A_i(\tau, \mathbf{x}_T)$, compute the spinor $\psi_{(3)}(\tau, z, \mathbf{x}_T)$ from the Dirac

equation using these color fields and the initial condition Eq. (16), project to a positive energy state $e^{-ip\cdot x}u(p)$ and, finally, integrate the square of the amplitude so obtained over momenta. As this is a rather involved operation, we shall first simplify the problem by neglecting the transverse dimension. Computation of $\mathrm{q\bar{q}}$ production in this 1+1 dimensional toy model permits us to test numerical aspects of the solution and the projection to final states. We shall return to the 3+1 dimensional case in future work.

As a first step, setting $U_{(m)}(\mathbf{x}_T) = 1$, $U_{(m)}(\mathbf{k}_T) = (2\pi)^2\delta^2(\mathbf{k}_T)$, in Eq. (16) gives

$$\psi_{(3)}(\tau = 0, z, \mathbf{x}_T)|_{U=1} = e^{-i\mathbf{q}_T\cdot\mathbf{x}_T}\Big[\, e^{iq^+x^-}P^+ - \frac{m}{\omega_q}e^{-y_q}\big(e^{iq^+x^-} - 1\big)\gamma^0P^+ \\ + e^{iq^-x^+}P^- - \frac{m}{\omega_q}e^{y_q}\big(e^{iq^-x^+} - 1\big)\gamma^0P^-\Big]v(q) \qquad (17)$$

This also illustrates the structure of Eq. (16): the left branch (first line) has for $z < 0$ (on the x^--axis) firstly a component $P^+v(q)$ moving in the $+z$ direction, but one also needs a component $\sim \gamma^0P^+v(q)$ to satisfy the Dirac equation. This is worked out explicitly below in Eq. (29). For $z > 0$ (on the x^+ axis) only $e^{-i\mathbf{q}_T\cdot\mathbf{x}_T}P^+v(q)$ moving in $+z$ direction remains. The right branch behaves symmetrically.

3 Free Dirac equation in 1+1 dimensions; analytic

Let us first define our spinor conventions and study the solutions of the free Dirac equation in 1+1 dimensions.

In 1+1 dimensions, given fermions of mass m, we can parametrise an on-shell momentum vector by just the rapidity y: $(E, p^z) = m(\cosh y, \sinh y)$. A free wave is then $e^{ip\cdot x} = e^{im\tau\cosh(y-\eta)}$.

Let us choose for the Dirac matrices a representation where $\gamma^0\gamma^3$ is diagonal:

$$\gamma^0 = \sigma^1 = \begin{pmatrix} 0 & 1 \\ 1 & 0 \end{pmatrix}, \quad \gamma^3 = -i\sigma^2 = \begin{pmatrix} 0 & -1 \\ 1 & 0 \end{pmatrix}, \quad \gamma^0\gamma^3 = \sigma^3 = \begin{pmatrix} 1 & 0 \\ 0 & -1 \end{pmatrix}. \qquad (18)$$

In this basis the projection operators defined in Eq. (1) are simply:

$$P^+ = \begin{pmatrix} 1 & 0 \\ 0 & 0 \end{pmatrix}, \quad P^- = \begin{pmatrix} 0 & 0 \\ 0 & 1 \end{pmatrix}, \qquad (19)$$

and we denote the two components by $\psi^\pm$:

$$\psi = \begin{pmatrix} \psi^+ \\ \psi^- \end{pmatrix}. \qquad (20)$$

The Dirac equation:

$$(i\gamma^\mu\partial_\mu - m)\,\psi = 0 \qquad (21)$$

has plane wave solutions corresponding to positive and negative energy:

$$\psi_{(+)}(x) = e^{-ip\cdot x}u(y) \quad \psi_{(-)}(x) = e^{ip\cdot x}v(y). \tag{22}$$

Using the explicit forms of the Dirac matrices we can easily see that

$$u(y) = \sqrt{m}\begin{pmatrix} e^{\frac{1}{2}y} \\ e^{-\frac{1}{2}y} \end{pmatrix}, \quad v(y) = \sqrt{m}\begin{pmatrix} e^{\frac{1}{2}y} \\ -e^{-\frac{1}{2}y} \end{pmatrix}. \tag{23}$$

The solutions have a Lorentz-invariant normalisation with $\overline{u}(y)u(y) = \overline{v}(y)v(y) = 2m$ and $\overline{u}(y)v(y) = \overline{v}(y)u(y) = 0$. The quantity we will be interested in, however, is the particle number density on a constant proper time surface, which is the τ–component of a Lorentz vector. For both the positive and negative energy solutions it is given by $\overline{u}(y)\gamma^\tau u(y) = \overline{v}(y)\gamma^\tau v(y) = 2m\cosh(y-\eta)$. The cross term $\overline{u}(y)\gamma^\tau v(y) = 2m\sinh(y-\eta)$ is not zero, but vanishes by symmetry when integrated over the longitudinal coordinate η.

Writing the free Dirac equation in terms of $\psi^\pm = P^\pm\psi$, the eigenvectors of $\gamma^0\gamma^3$, we have

$$i\left(\partial_\tau + \frac{\partial_\eta}{\tau}\right)\psi^\pm = me^{\pm\eta}\psi^\mp, \tag{24}$$

or, squaring to get a second order equation,

$$\left[{\partial_\tau}^2 + \frac{1}{\tau}\partial_\tau - \frac{{\partial_\eta}^2}{\tau^2} + m^2\right]\psi^\pm = 0. \tag{25}$$

With an ansatz $\psi^\pm(\tau,\eta) = e^{n\eta}\psi_n^\pm(\tau)$ this reduces to the Bessel equation. The solutions that are separable and finite for $\tau = 0$ are of the form $e^{n\eta}J_n(m\tau)$.

To find the right linear combination of the separable solutions we have to look at the initial condition. This can be done by looking at the full initial condition, Eq. (16), and removing all the transverse degrees of freedom. One first takes $U_{(m)}(\mathbf{x}_T) = 1$, which leads to Eq. (17), and further sets $\mathbf{q}_T = 0$ and thus reduces ω_q to m. Using the 2d representation of γ^0, γ^3 and $v(q)$ given above, Eq. (17) then becomes [6]

$$\psi(\tau=0,z) = \sqrt{m}\begin{pmatrix} e^{y/2}e^{ime^y(|z|-z)/2} \\ -e^{-y/2}(e^{ime^y(|z|-z)/2}-1) \end{pmatrix} + \sqrt{m}\begin{pmatrix} e^{y/2}\left(e^{ime^{-y}(|z|+z)/2}-1\right) \\ -e^{-y/2}e^{ime^{-y}(|z|+z)/2} \end{pmatrix}, \tag{26}$$

where the first(second) term is the left(right) branch in Fig. 1. From this we find that the initial condition for, for example, the upper component of the left hand branch, must behave, up to a sign, for $\tau \to 0$ as:

$$\psi^+(\tau\to 0,\eta) = -\sqrt{m}e^{y/2}e^{i\frac{1}{2}m\tau e^{y-\eta}} = -\sqrt{m}e^{y/2}e^{i\frac{1}{2}me^y(\sqrt{\tau^2+z^2}-z)}. \tag{27}$$

[6] We will actually change the sign of this expression; this would correspond to changing the sign of $v(q)$ in Eq. (23), which is just a convention.

Such a solution can be constructed as a sum of Bessel function modes as

$$\psi^+(\tau,\eta) = -\sqrt{m}e^{y/2}\sum_{n=0}^{\infty}(ie^{y-\eta})^n J_n(m\tau); \tag{28}$$

using $J_n(m\tau) \to (m\tau/2)^n/n!$ for $\tau \to 0$ and summing over n gives Eq. (27). Using Eq. (24) we see that the other component of the spinor is:

$$\psi^- = \sqrt{m}e^{-y/2}\sum_{n=1}^{\infty}(ie^{y-\eta})^n J_n(m\tau), \tag{29}$$

which is exactly the same as the lower component of the first term in Eq. (26), showing the consistency of the approach. We show in Appendix B that when this wave function is projected on positive energy states, one obtains the same result ($\pm i/\cosh\frac{1}{2}(y-y')$ for the two branches) for the amplitude as from evaluating the Feynman diagrams in Fig. 2 or by specialising the Abelian amplitude in Eq. (15) to 2d.

4 Free Dirac equation in 1+1 dimensions; numerical

Let us now formulate the discretised solution of the Dirac equation using the coordinates τ, z. The advantage of this coordinate system is that it allows a simultaneous and symmetric treatment of both two branches. On the other hand, at $\tau = 0$, $\sqrt{2}x^{\pm} = |z| \pm z$ is not a continuous function of z and there are corresponding discontinuities in ψ. The free Dirac equation in this coordinate system is

$$\partial_\tau \psi^{\pm} = \frac{\sqrt{\tau^2+z^2}\pm z}{\tau}\left(\mp\partial_z\psi^{\pm} - im\psi^{\mp}\right) . \tag{30}$$

The initial condition for the left hand branch is:

$$\psi^+(\tau=0,z) = -e^{y/2}\exp\left(i\frac{me^y}{2}(|z|-z)\right) , \tag{31}$$

$$\psi^-(\tau=0,z) = e^{-y/2}\left[\exp\left(i\frac{me^y}{2}(|z|-z)\right)-1\right] , \tag{32}$$

and for the other one:

$$\psi^+(\tau=0,z) = e^{y/2}\left[1-\exp\left(i\frac{me^{-y}}{2}(|z|+z)\right)\right] , \tag{33}$$

$$\psi^-(\tau=0,z) = e^{-y/2}\left[\exp\left(i\frac{me^{-y}}{2}(|z|+z)\right)\right] . \tag{34}$$

Because the z-dependent coefficients in the equation would make any explicit scheme unstable, we discretise Eq. (30) implicitly[7]:

$$\begin{aligned}
&\frac{1}{2\mathrm{d}\tau}\left[\psi^{\pm}(\tau+\mathrm{d}\tau,z)-\psi^{\pm}(\tau-\mathrm{d}\tau,z)\right]\\
&\quad=\mp\frac{\sqrt{\tau^2+z^2}\pm z}{4\tau\mathrm{d}z}\Big[\psi^{\pm}(\tau+\mathrm{d}\tau,z+\mathrm{d}z)+\psi^{\pm}(\tau-\mathrm{d}\tau,z+\mathrm{d}z)\\
&\qquad-\psi^{\pm}(\tau+\mathrm{d}\tau,z-\mathrm{d}z)-\psi^{\pm}(\tau-\mathrm{d}\tau,z-\mathrm{d}z)\Big]-im\frac{\sqrt{\tau^2+z^2}\pm z}{\tau}\psi^{\mp}(\tau,z)\,. \quad (35)
\end{aligned}$$

Now the $\pm$-components are stored at different timesteps: $\psi^{+}(\tau)$; $\psi^{-}(\tau+\mathrm{d}\tau)$. This saves memory compared to storing the spinor at two timesteps, while the discretisation is still second order accurate in $\mathrm{d}\tau$. It seems that it is critical for the stability of the algorithm to also discretise the endpoints to second order accuracy in $\mathrm{d}z$. Thus, when in Eq. (35) we have used the centered difference

$$f'(z)\approx\frac{1}{2\,\mathrm{d}z}\left[f(z+\mathrm{d}z)-f(z-\mathrm{d}z)\right], \quad (36)$$

for the points inside the lattice, for the edges of the lattice Eq. (35) must be modified to use a one-sided second order accurate difference:

$$f'(z)\approx\frac{1}{\mathrm{d}z}\left[2f(z+\mathrm{d}z)-\frac{1}{2}f(z+2\mathrm{d}z)-\frac{3}{2}f(z)\right]. \quad (37)$$

This prescription could be described as a free boundary condition. Note that it would be quite unphysical to impose periodic boundary conditions in the z-direction. Technically this shows up e.g. in the fact that the coefficient in front of the ∂_z-term in Eq. (30) would be discontinuous at such a periodic boundary.

Eq. (35) forms a system of linear equations for $\psi^{\pm}(\tau+\mathrm{d}\tau)$ in terms of the known values $\psi^{\pm}(\tau-\mathrm{d}\tau)$ and $\psi^{\mp}(\tau)$. The system is almost tridiagonal and can be efficiently solved using LU-decomposition, leading to an algorithm which is slower than the corresponding explicit discretisation only by a constant factor.

After having solved numerically the Dirac equation to find the spinor at some finite proper time τ, we must project out the positive energy part of the wavefunction to find the amplitude for production of a pair at rapidities y, y'. This is given by

$$M(y',y)=\tau\int\frac{\mathrm{d}z}{\sqrt{\tau^2+z^2}}\overline{u}(y')\exp\left(im\left[\sqrt{\tau^2+z^2}\cosh y'-z\sinh y'\right]\right)\gamma^{\tau}\psi(\tau,z), \quad (38)$$

where

$$\gamma^{\tau}=\gamma^0e^{-\eta\gamma^0\gamma^3}=\gamma^0\left(\cosh\eta-\gamma^0\gamma^3\sinh\eta\right)=\gamma^0\left(\frac{\sqrt{\tau^2+z^2}}{\tau}-\gamma^0\gamma^3\frac{z}{\tau}\right) \quad (39)$$

and $\tau/\sqrt{\tau^2+z^2}$ is the Jacobian.

[7]The discretisation of a partial differential equation is said to be "implicit" when the time derivative of the unknown function at a given timestep depends on the unknown function at the next timestep.

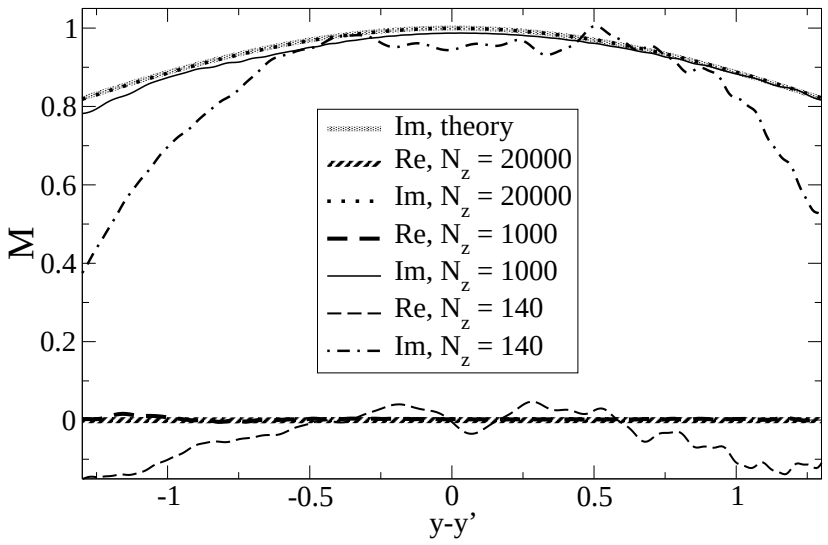

Figure 3: Numerically calculated real and imaginary parts of the free amplitude M for one branch shown for different lattice sizes in the z-direction. Also shown is the analytical value $1/\cosh(y-y')$ of the imaginary part. The analytical value of the real part is zero.

In practice the integral, or sum in the discrete case, is an oscillatory function for large z. In an analytical integration these oscillations average to zero, but in a numerical calculation with a finite extent in the z-direction this is harder to achieve. We have used two different techniques to treat this problem. One is to calculate the integral (38) for different upper and lower limits $\pm z_{\max}$, and then take an average of the values thus obtained over a range in $z_{\max}$ that contains several periods of oscillation. The other technique is to use wave packets which are localised in the z-direction to slightly less than the extent of the system in the z-direction. This introduces an uncertainty to the momentum in the z-direction or equivalently the rapidity y, but the uncertainty is of the same order of magnitude as the infrared cutoff from the size of the z-lattice.

The range of rapidity y that can be reached in this coordinate system is limited by two things. The finite lattice spacing in the z-direction gives an ultraviolet cutoff for p^z, implying that we must have $\sinh y \lesssim 1/(m\mathrm{d}z)$. Our method also requires that the values of η of the order of the momentum space rapidities studied be covered by the finite lattice in the z-direction. This translates into the requirement $\sinh y \lesssim z_{\max}/\tau$. Fig. 3 gives an idea of how close our results are to the analytically known result (for one branch) $M(y', y) = i/\cosh\frac{1}{2}(y - y')$ (see Appendix B).

5 Dirac equation in 1+1 dimensions; external field

First let us note that this is not a calculation of pair production from the Weizsäcker-Williams fields of two currents on the light cone, because such a thing does not exist in two spacetime dimensions. Assuming an external current

$$J^+ = e_1\delta(x^-), \quad J^- = e_2\delta(x^+),$$

one can namely solve $\partial_\mu F^{\mu\nu} = J^\nu$ for the only component $E = F^{+-}$ to be $E = -e_1\Theta(x^-) + e_2\Theta(x^+)$. There is just a constant electric field off the light cone. Instead, our purpose is to impose by hand an external field to test our numerical method and to model the projection of the real 3+1 dimensional physics on the longitudinal dimension. The parameters of the calculation will be m, the mass parameter of the Dirac equation, Q_s, another mass parameter describing the proper time variation of the external field and c, a dimensionless parameter describing the strength of the external field. To effectively describe the omitted transverse momentum effects one might take m to be not very different from Q_s. For $c \ll 1$ one is in the weak field domain and analytic results can be obtained.

With the gauge choice $A_\tau = 0$ and an external gauge field $A_\eta(\tau)$ the Dirac equation (30) becomes:

$$\partial_\tau\psi^\pm = \frac{\sqrt{\tau^2+z^2} \pm z}{\tau}\left(\mp\partial_z\psi^\pm - im\psi^\mp\right) \mp i\frac{gA_\eta(\tau)}{\tau}\psi^\pm. \tag{40}$$

We shall study this for various choices of $A_\eta(\tau)$. The first choice, motivated by the perturbative solution of the Yang-Mills equations[7] is

$$gA_\eta(\tau) = cQ_\mathrm{s}\tau J_1(Q_\mathrm{s}\tau). \tag{41}$$

This form is special in that the Fourier transformed fields corresponding to (41) can be given analytically:

$$gA^\pm(k^+,k^-) = \pm cQ_\mathrm{s}^2\frac{i}{k^\mp + i\epsilon}\,\frac{1}{2k^+k^- - Q_\mathrm{s}^2 + i\epsilon(k^+ + k^-)}. \tag{42}$$

Note that the pole structure is dictated by the requirement that $A^\mu \sim \theta(x^+)\theta(x^-)$. Using this explicit form for the field in (41) and the spinors in (23) one can write the lowest order perturbative result (corresponding to diagram (a) in Fig. 5) for the amplitude:

$$M = -ig\overline{u}(p)\not{A}(p+q)v(q) \tag{43}$$

in the form

$$M(\Delta y \equiv y - y') = \frac{2cQ_\mathrm{s}^2}{\cosh(\frac{1}{2}\Delta y)\,[2m^2(1+\cosh\Delta y) - Q_\mathrm{s}^2 + i\epsilon]} \equiv \frac{2cQ_\mathrm{s}^2}{\cosh(\frac{1}{2}\Delta y)\,[\hat{s} - Q_\mathrm{s}^2 + i\epsilon]}. \tag{44}$$

Numerical results for the field (41) are shown in Fig. 4 at a fixed large time $\tau = N_\tau d\tau$, the time dependence is studied in Fig. 6. In Fig. 4 the left panel shows the amplitude for weak

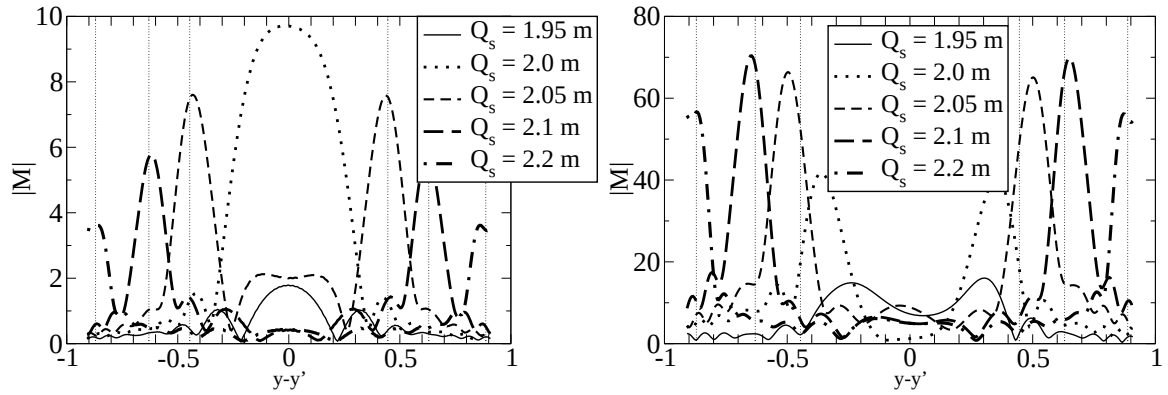

Figure 4: Absolute value of the quark pair production amplitude for different values of the oscillation scale Q_s. Left: weak fields ($cQ_\mathrm{s} = 0.05m$), the peaks are at the location given by Eq. (45). Right: strong fields ($cQ_\mathrm{s} = m$) with the same values of Q_s. Peaks near the "threshold" $Q_\mathrm{s} = 2m$ are shifted.

fields and the right one for strong fields. For weak fields, $c \ll 1$, one expects the numerical result to coincide with first order perturbation theory, as given by (44), which has a peak at $\hat{s} = Q_\mathrm{s}^2$ or at

$$\cosh \frac{\Delta y}{2} = \frac{Q_\mathrm{s}}{2m}. \tag{45}$$

For $Q_\mathrm{s} < 2m$ this equation has no solution for Δy and, in fact, the numerical result is very small. Precisely at "threshold", $Q_\mathrm{s} = 2m$, there is a very strong single peak at $\Delta y = 0$, the quark and antiquark emerge at rest relative to each other. For $Q_\mathrm{s} > 2m$ there are two peaks corresponding to the two signs of solutions of (45). These are well reproduced by the numerical calculation. Due to the finite time the peak is not a delta function, but is broadened. Physically, the amplitude peaks at pair invariant mass $= Q_\mathrm{s}$ and, in 1+1d, the only way to give the pair this invariant mass is to separate them in rapidity. In 3+1d the situation is quite different, since then

$$\hat{s} \equiv (p+q)^2 = 2\omega_p \omega_q \cosh \Delta y + 2m^2 - 2\mathbf{p}_T \cdot \mathbf{q}_T \tag{46}$$

and the pair invariant mass can even be dominated by transverse momenta.

For stronger fields the numerical calculation sums over all orders in the external field (all diagrams in Fig. 5) and one does not necessarily expect any peak structure. However, peaks still appear (right panel of Fig. 4), although the location of the peaks is shifted, especially near $Q_\mathrm{s} = 2m$.

Fig. 6 shows the dependence on the physical time $\tau = N_\tau \mathrm{d}\tau$, at which the projection to the final state is done. One sees that the height of the peaks increases essentially linearly in time, $M_\mathrm{peak} \sim N_\tau$, while their widths shrink somewhat. The area of each of the peaks, $\int \mathrm{d}y |M|$, is approximately independent of N_τ, showing that the resulting rapidity distribution at asymptotic times contains two delta function peaks in Δy. The right panel shows that the

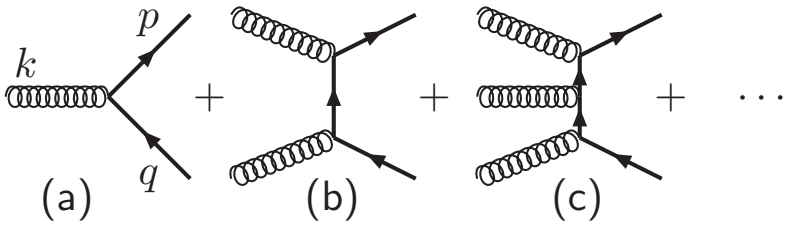

Figure 5: Diagrams contributing to the amplitude in the 1+1-dimensional toy model.

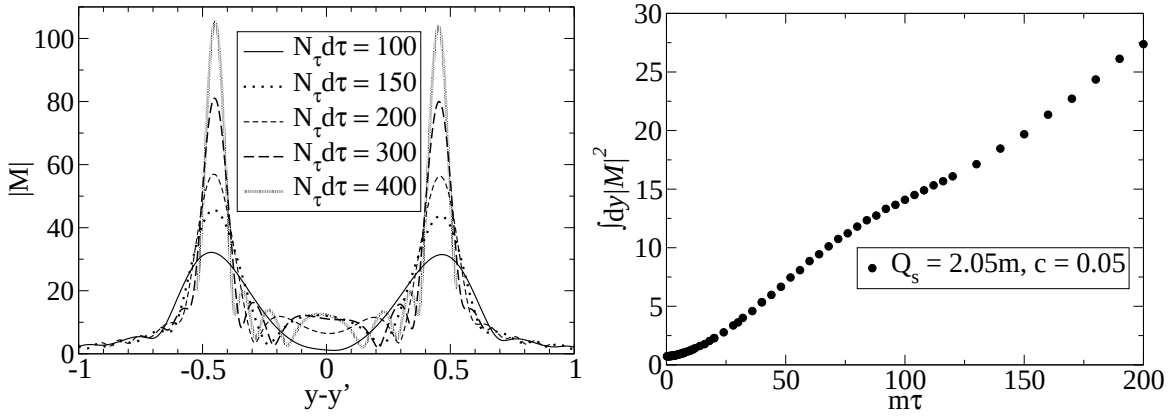

Figure 6: Left: Absolute value of the amplitude for $Q_\mathrm{s} = 2.05m$ and $cQ_\mathrm{s} = 0.5m$ when the projection is made at different physical times $N_\tau d\tau$ at a fixed $d\tau = 0.05/m$. Right: The number of produced pairs per unit rapidity, $\int \mathrm{d}\Delta y |M|^2$, as a function of time. Note that $Q_\mathrm{s} > 2m$, so that the delta-function peak in Eq. (44) dominates.

integral $\int \mathrm{d}y|M|^2$, giving the number of produced pairs, grows approximately linearly with τ. This monotonic increase is due to the fact that the ansatz of Eq. (41) behaves like $\sim \sqrt{\tau}$ at large τ.

As a second example we shall consider a non-oscillatory and exponentially decaying field

$$gA_\eta(\tau) = cQ_\mathrm{s}\tau e^{-Q_\mathrm{s}\tau}. \tag{47}$$

This is actually simply reproduced from the first ansatz of Eq. (41) by taking a superposition of Bessel functions $\omega\tau J_1(\omega\tau)$ with different frequencies ω, which "washes out" the peaks at $\hat{s} = \omega^2$ in (44). The appropriate weight factor is given by the relation

$$gA_\eta(\tau) = c\int_0^\infty \mathrm{d}\omega \frac{Q_\mathrm{s}\omega}{(\omega^2 + Q_\mathrm{s}^2)^{3/2}} \omega\tau J_1(\omega\tau) = cQ_\mathrm{s}\tau e^{-Q_\mathrm{s}\tau}. \tag{48}$$

Integrating over the matrix element (44) (with $Q_\mathrm{s} \to \omega$) one finds the perturbative matrix

element

$$M(\Delta y) = -\frac{cQ_{\rm s}\hat{s}}{\cosh(\frac{1}{2}\Delta y)(\hat{s}+Q_{\rm s}^2)^{3/2}}\left\{i\pi + 2\left[\frac{Q_{\rm s}^2}{\hat{s}}\sqrt{1+\frac{\hat{s}}{Q_{\rm s}^2}} + \ln\left(\sqrt{1+\frac{Q_{\rm s}^2}{\hat{s}}}+\sqrt{\frac{Q_{\rm s}^2}{\hat{s}}}\right)\right]\right\} \tag{49}$$

Now there is no peak at $\hat{s} = Q_{\rm s}^2$ and, when plotted as a function of Δy for various $Q_{\rm s}/m$, $M(\Delta y)$ is a Gaussian-like curve centered around $\Delta y = 0$.

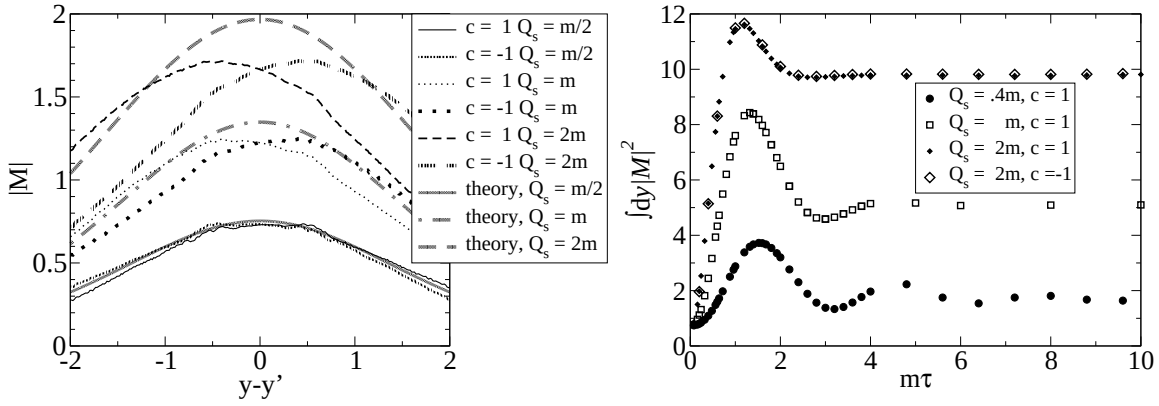

Figure 7: Left: Numerically computed amplitude for the strong ($c = \pm 1$) exponentially decaying field in Eq. (48). The curves labeled "theory" are the weak field analytical result from Eq. (49). Changing $c \to -c$ reflects the curves around $\Delta y = 0$. Right: The number of produced pairs per unit rapidity, $\int {\rm d}\Delta y |M|^2$, as a function of time for the exponentially decaying field.

Numerical results for the amplitude for $Q_{\rm s} \sim m$ and a strong field $c = \pm 1$ are shown in the left panel of Fig. 7. The general form of the rapidity dependence and the normalisation agree quite well with the weak field formula (49), but the numerical curves are not centered exactly around $\Delta y = 0$. This asymmetry under $\Delta y \to -\Delta y$ is simply due to the fact that under parity $A_\eta \to -A_\eta$ and thus the ansatz (47) (as well as any non-zero A_η) breaks parity. To check that this is a real physical effect the numerical calculations have been performed with both $c = 1$ and $c = -1$. In the Dirac equation this corresponds to $z \to -z$ and $\Delta y \to -\Delta y$ and the curves obtained agree with this. The right panel of Fig. 7 shows the number of pairs produced, $\int {\rm d}\Delta y |M|^2$. Initially it rises $\sim Q_{\rm s}\tau$, then after a few oscillations, caused by the coupling of the two frequency scales $Q_{\rm s}$ and m, reaches a constant multiplicity level. $Q_{\rm s}$ being a timescale of damping, the oscillation frequency is given by m. The larger $Q_{\rm s}/m$, the larger is the multiplicity. This constancy is due to the fact that the external field vanishes in a time $\sim 1/Q_{\rm s}$.

6 Numerical tests

Because of the delicate nature of the time-longitudinal dynamics, we have performed various tests of the numerics. In Fig. 8 we study the effect of taking different (physical) sizes for the lattice in the z-direction, or $z_{\max}$, using the Bessel function external field (41). Especially when the projection is done at a larger time the amplitude depends somewhat on the size of the lattice. The difference in the multiplicity $\int \mathrm{d}y|M|^2$ is, however, quite small. For the exponentially decaying field (47) the lattice size effect is much smaller, almost unobservable on a plot like Fig. 8. The effect of a finite $z_{\max}$ on the integral $\int \mathrm{d}y|M|^2$ is larger for the exponentially decaying field, because of the contribution from larger values of $|\Delta y|$ that are unaccessible for a small $z_{\max}$ (see the discussion at the end of Sec. 4).

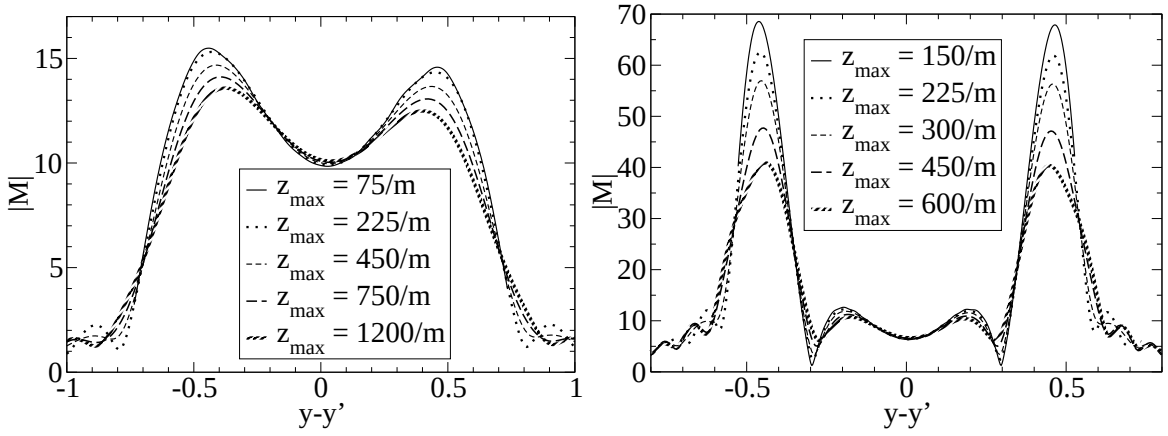

Figure 8: Absolute value of the amplitude for different sizes of the lattice size in the z-direction. The external field is a Bessel function Eq. (41) with a frequency slightly above the resonance condition, $Q_{\mathrm{s}} = 2.05m$. Left: $cQ_{\mathrm{s}} = 0.615m$ and $N_\tau \mathrm{d}\tau = 60/m$. Right: $cQ_{\mathrm{s}} = 0.5m$ and $N_\tau \mathrm{d}\tau = 100/m$. There is some dependence on the lattice size, and the dependence is larger when the projection is done at a later time (right panel).

The left panel of Fig. 9 shows the dependence on the timestep used. In the right panel of Fig. 9 we choose different rapidities y for the antiquark and compute the distribution in the quark rapidity y'. The outcome is always a function of $y - y'$, which shows that our numerical method preserves the boost invariance of the result to a good accuracy. In Fig. 10 we explore the accuracy that can be reached with lattices small enough to make a full 3+1-dimensional computation realistic. Although the computational requirements of a 3+1d-simulation are quite hard, we believe that with a careful choice of discretisation parameters it is possible to extract some physical results from a full 3+1d numerical calculation.

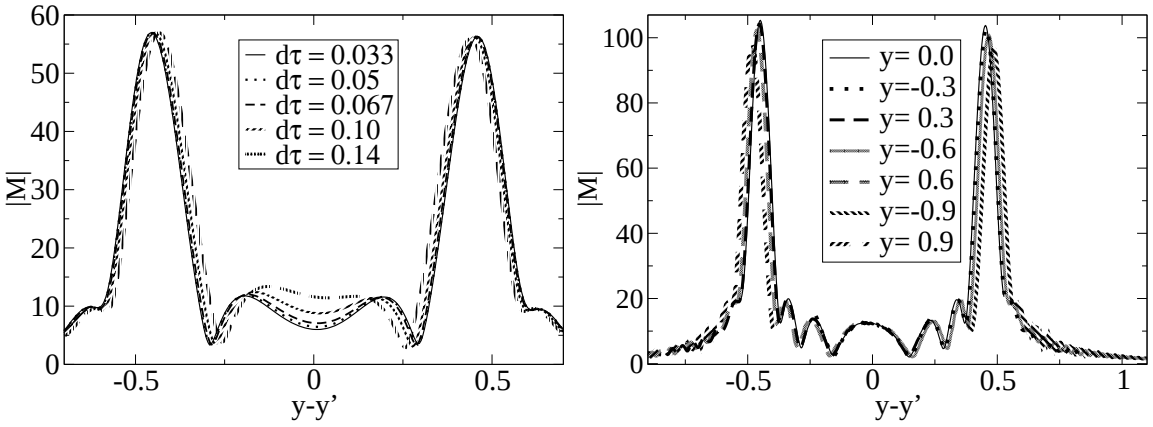

Figure 9: Left: Absolute value of the amplitude using different timesteps at fixed physical size $N_\tau d\tau = 400/m$. Right: amplitude for different values of the antiquark rapidity y; to check that the numerical calculation reproduces the boost invariance of the solution. Both plots have an oscillating field with $Q_\mathrm{s} = 2.05m$ and $cQ_\mathrm{s} = 0.5m$ but different lattice sizes in the z-direction.

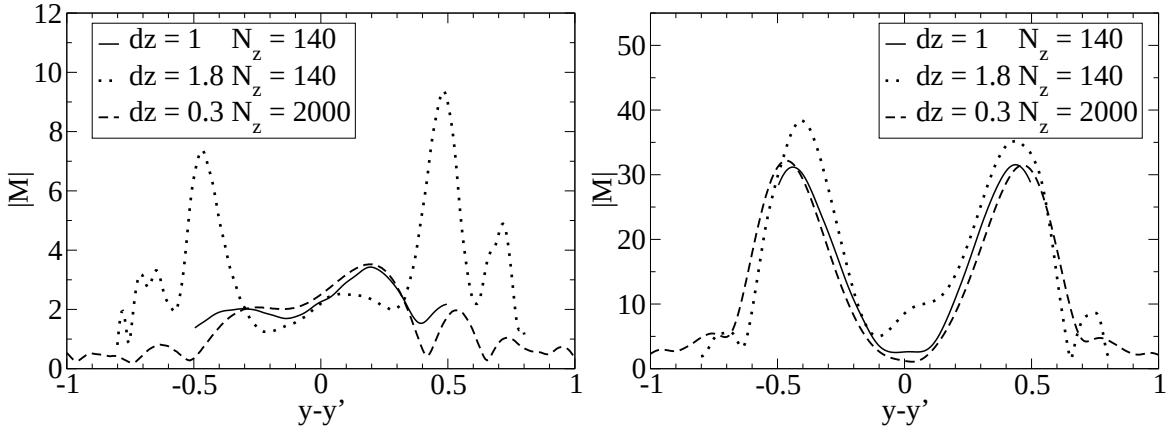

Figure 10: Absolute value of the amplitude for smaller lattice sizes in the z-direction. Left: Q_s below resonance ($Q_\mathrm{s} = m$ and $cQ_\mathrm{s} = m$). Right: Q_s above resonance ($Q_\mathrm{s} = 2.05m$ and $cQ_\mathrm{s} = 0.5m$). Values of z in units of $[1/m]$.

7 Conclusions

In this paper, we have set up the framework for computing $\mathrm{q\bar{q}}$ pair production in ultrarelativistic heavy ion collisions in the classical field model with an ensemble of quantum initial conditions. This is an important theoretical problem, especially in view of nonperturbative chemical thermalisation, for which one needs a sufficient number of $\mathrm{q\bar{q}}$ pairs from the dominantly gluonic initial state. However, the calculation is technically complicated, involving the

numerical solution of both the gauge field equations of motion and the Dirac equation in the background gauge field. Even the formulation of the initial condition proves to be nontrivial since the natural variables τ, η cannot in the limit $\tau \to 0$ give a dimensionful longitudinal variable, which one needs for longitudinal Fourier transforms. In view of this, we have in this paper limited ourselves to giving only the initial condition for the full 3+1d problem but considered in numerical detail only a 1+1d version of the model obtained after truncation of the transverse dynamics. In this model both rapidity distributions and the total number of produced pairs were computed for two forms of the gluonic external field.

The work carried out here has solved the conceptually most complicated part of the full 3+1d problem, the formulation of the initial condition and the treatment of the longitudinal dimension together with the proper time. The inclusion of transverse dynamics is computationally demanding but otherwise straightforward. When that part is completed, one will be in a position to make meaningful statements about the nonperturbative production of $\mathrm{q\bar{q}}$ pairs in heavy ion collisions.

Future tasks include a full 3+1-dimensional treatment of also the gauge field equations of motion and ultimately also including feedback from the $\mathrm{q\bar{q}}$ sector to gluons, i.e., formulating and solving coupled equations of motion. This will be a very challenging task.

Acknowledgements

This work was partly supported by the Academy of Finland, Contract no. 77744 and the European Community Integrated Infrastructure Initiative Project "Study of Strongly Interacting Matter" Contract No RII3-CT-2004-506078. T.L. was supported by the Magnus Ehrnrooth Foundation and the Finnish Cultural Foundation. We wish to thank J.P. Blaizot, D. Dietrich, E. Iancu, L. McLerran, A. Peshier, K. Tuchin and R. Venugopalan for discussions on this and closely related issues.

A Dirac equation in curved coordinates

Let us denote the flat coordinates t, z or x^0, x^3 by Latin indices $a, b, \ldots$ and the curved ones τ, η by Greek ones: $\mu, \nu, \ldots$. The flat metric is $\eta_{ab} = \mathrm{diag}(1, -1)$ and the curved one $g_{\mu\nu} = \mathrm{diag}(1, -\tau^2)$, $g^{\mu\nu} = \mathrm{diag}(1, -1/\tau^2)$. The nonzero Christoffel symbols for the τ, η coordinates are [27] $\Gamma^{\tau}_{\eta\eta} = \tau$ and $\Gamma^{\eta}_{\tau\eta} = \Gamma^{\eta}_{\eta\tau} = 1/\tau$.

Given some representation for the usual γ-matrices in flat space, γ^a, one can express the γ-matrices in curved coordinates as $\gamma^\mu = e^\mu_a \gamma^a$. The *zweibein* e^μ_a relates the flat metric to the curved one by $g_{\mu\nu} = e^a_\mu e^b_\nu \eta_{ab}$ and, conversely, $\eta_{ab} = e^\mu_a e^\nu_b g_{\mu\nu}$. There is no unique choice for the e^μ_a, reflecting the fact that there are different ways one can attach a flat tangent space to each point in spacetime. We have mostly used the natural intuitive choice for the *zweibein*, namely $e^a_\mu = \partial_\mu x^a$. But in the τ, η-coordinate system there is also another natural choice,

namely to take $e^0_\tau = 1$, $e^3_\eta = \tau$, so that γ^μ do not depend on the coordinates. To preserve the local Lorentz invariance of the Dirac equation, one must introduce a *spin connection*[19]:

$$\Gamma_\mu = \frac{1}{8}[\gamma^a, \gamma^b] e_{\nu a}(\partial_\mu e^\nu_b + \Gamma^\nu_{\mu\sigma} e^\sigma_b). \tag{50}$$

In this case the spin connection has only one nonvanishing component:

$$\Gamma_\eta = \frac{1}{2}\gamma^0\gamma^3. \tag{51}$$

The free Dirac equation $[i\gamma^\mu(\partial_\mu + \Gamma_\mu) - m]\,\widetilde{\psi} = 0$ in this case becomes:

$$\left[i\left(\gamma^0\partial_\tau + \frac{\gamma^3}{\tau}\partial_\eta + \frac{\gamma^0}{2\tau}\right) - m\right]\widetilde{\psi} = 0. \tag{52}$$

Here we have introduced the spinor $\widetilde{\psi}$ defined with this choice of the *zweibein*. It is related to the usual flat space spinor by $\widetilde{\psi} = e^{-\frac{1}{2}\eta\gamma^0\gamma^3}\psi$. The plane wave solutions (22) and (23) now have a form that makes boost invariance manifest:

$$\widetilde{\psi}_{(\pm)}(x) = \sqrt{m}e^{\mp im\tau\cosh(y-\eta)}\begin{pmatrix} e^{\frac{1}{2}(y-\eta)} \\ \pm e^{\frac{1}{2}(\eta-y)}\end{pmatrix}. \tag{53}$$

B Amplitude

We found that the solution of the free Dirac equation for the left branch in Fig. 1 in the future light cone is (Eqs. (28) and (29))

$$\psi^+ = -\sqrt{m}e^{y/2}\sum_{n=0}^{\infty}(ie^{y-\eta})^n J_n(m\tau) \tag{54}$$

$$\psi^- = \sqrt{m}e^{-y/2}\sum_{n=1}^{\infty}(ie^{y-\eta})^n J_n(m\tau). \tag{55}$$

To project to a positive energy state with rapidity y', we calculate the amplitude

$$M_1(y', y) = \tau\int \mathrm{d}\eta\,\overline{u}(y')e^{im\tau\cosh(\eta-y')}\gamma^\tau\psi(\tau,\eta). \tag{56}$$

Inserting the form (54) and using the standard integral

$$\int_{-\infty}^{\infty}\mathrm{d}\eta\,e^{i\zeta\cosh(\eta-y)-\nu\eta} = e^{-\nu y}i\pi e^{i\nu\pi/2}H^{(1)}_\nu(\zeta) \tag{57}$$

and the Wronskian relation

$$H^{(1)}_n(m\tau)J_{n+1}(m\tau) - H^{(1)}_{n+1}(m\tau)J_n(m\tau) = \frac{2i}{\pi m\tau} \tag{58}$$

one gets

$$M_1(y', y) = \frac{-i}{\cosh \frac{y-y'}{2}}. \tag{59}$$

The other right branch has the initial condition

$$\psi^- = \sqrt{m} e^{-y/2} \sum_{n=0}^{\infty} (ie^{\eta - y})^n J_n(m\tau) \tag{60}$$

$$\psi^+ = -\sqrt{m} e^{y/2} \sum_{n=1}^{\infty} (ie^{\eta - y})^n J_n(m\tau) \tag{61}$$

and leads to a contribution which exactly cancels that from the left branch:

$$M_2(y', y) = \frac{i}{\cosh \frac{y-y'}{2}}. \tag{62}$$

These two contributions and the way they cancel are exactly the same that come from evaluating, in 1+1 dimensions, the Feynman diagrams in Fig. 2.

References

[1] For a review of RHIC data, see Proceedings of Quark Matter 2004, J. Phys. G **30**, S633-S1429 (2004)

[2] K. H. Ackermann *et al.* [STAR Collaboration], Phys. Rev. Lett. **86** (2001) 402 [arXiv:nucl-ex/0009011].

[3] K. Adcox *et al.* [PHENIX Collaboration], Phys. Rev. Lett. **89** (2002) 212301 [arXiv:nucl-ex/0204005].

[4] B. B. Back *et al.* [PHOBOS Collaboration], Phys. Rev. Lett. **89** (2002) 222301 [arXiv:nucl-ex/0205021].

[5] P. F. Kolb, J. Sollfrank and U. W. Heinz, Phys. Rev. C **62** (2000) 054909 [arXiv:hep-ph/0006129].

[6] L. V. Gribov, E. M. Levin and M. G. Ryskin, Phys. Rept. **100** (1983) 1.

[7] A. Kovner, L. D. McLerran and H. Weigert, Phys. Rev. D **52** (1995) 6231 [arXiv:hep-ph/9502289]; A. Kovner, L. D. McLerran and H. Weigert, Phys. Rev. D **52** (1995) 3809 [arXiv:hep-ph/9505320].

[8] L. D. McLerran and R. Venugopalan, Phys. Rev. **D49**, 2233 (1994), [hep-ph/9309289].

[9] K. J. Eskola, K. Kajantie, P. V. Ruuskanen and K. Tuominen, Nucl. Phys. **B570**, 379 (2000), [hep-ph/9909456].

[10] M. Gyulassy and L. McLerran, "New forms of QCD matter discovered at RHIC," arXiv:nucl-th/0405013.

[11] P. Braun-Munzinger, D. Magestro, K. Redlich and J. Stachel, Phys. Lett. B **518** (2001) 41 [arXiv:hep-ph/0105229].

[12] D. M. Elliott and D. H. Rischke, Nucl. Phys. A **671** (2000) 583 [arXiv:nucl-th/9908004].

[13] A. Krasnitz and R. Venugopalan, Nucl. Phys. B **557** (1999) 237 [arXiv:hep-ph/9809433]; A. Krasnitz, Y. Nara and R. Venugopalan, Nucl. Phys. A **727** (2003) 427 [arXiv:hep-ph/0305112].

[14] T. Lappi, Phys. Rev. C **67** (2003) 054903 [arXiv:hep-ph/0303076].

[15] E. Iancu, A. Leonidov and L. McLerran, arXiv:hep-ph/0202270; E. Iancu and R. Venugopalan, arXiv:hep-ph/0303204.

[16] A. J. Baltz and L. D. McLerran, Phys. Rev. C **58**, 1679 (1998) [arXiv:nucl-th/9804042].

[17] A. J. Baltz, F. Gelis, L. D. McLerran and A. Peshier, Nucl. Phys. A **695** (2001) 395 [arXiv:nucl-th/0101024].

[18] K. Kajantie and T. Matsui, Phys. Lett. B **164** (1985) 373; G. Gatoff, A. K. Kerman and T. Matsui, Phys. Rev. D **36** (1987) 114.

[19] Y. Kluger, J. M. Eisenberg, B. Svetitsky, F. Cooper and E. Mottola, Phys. Rev. D **45** (1992) 4659; F. Cooper, J. M. Eisenberg, Y. Kluger, E. Mottola and B. Svetitsky, Phys. Rev. D **48** (1993) 190 [arXiv:hep-ph/9212206].

[20] F. Gelis and R. Venugopalan, Phys. Rev. D **69** (2004) 014019 [arXiv:hep-ph/0310090].

[21] D. D. Dietrich, Phys. Rev. D **68** (2003) 105005 [arXiv:hep-th/0302229]; D. D. Dietrich, arXiv:hep-th/0402026.

[22] G. Aarts and J. Smit, Nucl. Phys. B **555** (1999) 355 [arXiv:hep-ph/9812413].

[23] E. Shuryak and I. Zahed, Phys. Rev. D **67** (2003) 014006 [arXiv:hep-ph/0206022].

[24] R. N. Lee and A. I. Milstein, Phys. Rev. A **61** (2000) 032103 [arXiv:hep-ph/9909452].

[25] A. Krasnitz, Y. Nara and R. Venugopalan, Nucl. Phys. A **717** (2003) 268 [arXiv:hep-ph/0209269].

[26] A. H. Mueller, Phys. Lett. B **523**, 243 (2001) [arXiv:hep-ph/0110169]; K. Rummukainen and H. Weigert, Nucl. Phys. A **739** (2004) 183 [arXiv:hep-ph/0309306].

[27] A. Makhlin, Phys. Rev. C **63** (2001) 044902 [arXiv:hep-ph/0007300].